JOURNAL OF MATERIALS SCIENCE 29 (1994) 1227–1232

Structural properties of lead vanadate glasses containing La^{3+} or Fe^{3+} ions

S. MUSIĆ, M. GOTIĆ, S. POPOVIĆ,* K. FURIĆ, V. MOHAČEK
*Ruđer Bošković Institute, P. O. Box 1016, 41001 Zagreb, Republic of Croatia, * and also Department of Physics, Faculty of Science, University of Zagreb, P. O. Box 162, 41001 Zagreb, Republic of Croatia*

Structural properties of lead vanadate glasses containing La^{3+} or Fe^{3+} ions were investigated using X-ray diffraction, Fourier transform infrared spectroscopy and laser Raman spectroscopy. Crystalline $Pb_2V_2O_7$ was formed for the molar composition $66.7PbO–33.3V_2O_5$. Incorporation of greater quantities of La^{3+} into lead metavanadate glass caused the crystallization of $Pb_2V_2O_7$. Fourier transform infrared and laser Raman spectra also suggested the presence of $LaVO_4$. Incorporation of Fe^{3+} ions into lead metavanadate glass, up to 20 wt % Fe_2O_3, did not cause crystallization inside the glass matrix. Changes in the vibrational spectra are discussed.

1. Introduction

Mixed oxides of metal cations and vanadium are characterized by specific chemical and structural properties. These materials have found different applications (catalysis, dosimetry, luminescence devices, etc.) [1, 2]. Some vanadate glasses showed semiconducting properties [3]. The conduction in vanadate glasses was explained by the electron hopping between V^{5+} and V^{4+} through the V–O–V bonds. Partial reduction of V^{5+} to V^{4+} in the molten state was also observed for the system $CuO–V_2O_5$ [4], and this is assumed to be responsible for the semiconducting properties of copper vanadates. After the thermal treatment of V_2O_5, both V^{4+} and V^{3+} ions were found in V_2O_5, and the V^{4+} yield was greater than that of V^{3+} [5]. Oxygen deficiency appeared to be the original cause of the structural instability of V_2O_5.

The $PbO–V_2O_5$ system has also been extensively investigated. In the chemical sense, the $PbO–V_2O_5$ system is relatively simple; however, structurally, this system is of a complex nature. Depending on the PbO/V_2O_5 ratio, temperature of melting, mode and the time of quenching, in addition to the amorphous phase, different metastable and stable crystalline phases may be formed [6]. Slobodin *et al.* [7] investigated the $PbO–V_2O_5$ system and determined concentration regions and the temperatures for the formation of lead metavanadate, $Pb(VO_3)_2$, and lead pyrovanadate, $Pb_2V_2O_7$. The investigation of the equimolar $PbO–V_2O_5$ system showed [8, 9] the existence of two new lead metavanadate phases, which crystallized from the melt when the cooling rate was extremely high. These phases were embedded into glass matrix, and on heating they transformed to the well-known stable phase PbV_2O_6 [10]. Baiocchi *et al.* [11] also investigated the system $PbO–V_2O_5$ and they found two crystalline phases inside the glass matrix. On the basis of the X-ray diffraction (XRD) patterns, the authors suggested the existence of two different pyrovanadate phases, α-PbV_2O_7 and β-PbV_2O_7. Momo *et al.* [12] investigated the equimolar $PbO–V_2O_5$ system. Depending on the cooling rate from the melt, samples could be obtained either as amorphous or as polycrystalline lead metavanadate, PbV_2O_6, or as mixtures containing polycrystalline and amorphous phases. The samples contained 1.70%–2.16% V^{4+} in relation to the total vanadium. The appearance of very different ESR line shapes for differently prepared materials was explained by the difference in the hopping rate of the charge carriers. The magnetic properties of the semiconducting system PbV_2O_6 were investigated using glass, as well as the crystalline modification, obtained by a very fast or a very slow cooling, respectively [13]. The results of magnetic susceptibility measurements, performed in the temperature range $4.2 \leqslant T \leqslant 250$ K were reported. The differences between the observed magnetic behaviour were attributed to the different jumping rates of the 3d electrons for V^{4+} and V^{5+} states in the glass and crystalline samples. The magnetic properties of the glass phase were described in terms of a crystal field model for localized electrons, which, on the other hand, is inadequate for the crystalline phase, because of a higher electron mobility.

In the present work, the dependence of the formation of glass and crystalline phases in the $PbO–V_2O_5$ system on the kind of dopant ions, La^{3+} or Fe^{3+}, and their concentrations, was investigated. Structural changes in the samples were followed by X-ray diffraction, Fourier transform infrared (FT–IR) spectroscopy and laser Raman spectroscopy.

2. Experimental procedure

The chemicals, PbO, La_2O_3 and Fe_2O_3, were obtained from Ventron, while V_2O_5 was obtained from

0022–2461

Kemika, Zagreb. The experimental conditions employed for the preparation of the samples are given in Table I.

X-ray powder diffraction measurements were performed at room temperature using a Philips counter diffractomer with monochromatized CuK_α radiation (graphite monocromator).

FT–IR spectra were recorded at room temperature using a spectrometer 1720–x produced by Perkin–Elmer. Samples in powder form were pressed into discs using spectroscopically pure KBr.

Raman spectra were recorded using a DILOR Z24 triple monochromator with 514.5 nm line of COHERENT INNOVA-100 argon laser as excitation source. The power at the sample was 200 mW and the step size ranged from 0.5–2 cm^{-1}. Powder samples were pressed with KBr into pellets to improve the conduction of heat, which develops in the focus of the laser beam, away from the sample. Because of the opacity of the samples, a spinning cell and multiscanning technique had to be used.

3. Results and discussion

The results of X-ray diffraction phase analysis are given in Table II. For the molar composition 66.7PbO–33.3V_2O_5 (sample S-1) crystalline lead pyrovanadate, $Pb_2V_2O_7$, was detected. On the other hand, for the molar compositions 50.0PbO–50.0V_2O_5 (sample S-2) and 33.3PbO–66.7V_2O_5 (sample S-3), pure glasses were obtained. Samples S-4 and S-5, which contained 2.5 and 5.0 wt % La_2O_3, respectively, were completely in the glassy state, as shown by XRD. Incorporation of 10 wt % La_2O_3 into the glass with metavanadate composition induced crystallization of a small amount of $Pb_2V_2O_7$ (sample S-6). The crystallization of $Pb_2V_2O_7$ was more pronounced in sample S-7 which contained 20 wt % La_2O_3. However, when the temperature of the melt was increased (up to 1300 °C, sample S-8), a smaller molar fraction of crystallized $Pb_2V_2O_7$ was detected, in spite of fact that the La_2O_3 content was additionally increased to 25 wt %. Fig. 1 shows X-ray diffraction patterns of samples S-1, S-8 and S-6. Because there is an overlapping of the prominent X-ray diffraction lines of $Pb_2V_2O_7$ and $LaVO_4$, the presence of $LaVO_4$ in glasses with higher contents of La_2O_3 cannot be excluded. Lead metavanadate glasses doped with Fe_2O_3 up to 20 wt % were completely amorphous (samples S-9, S-10, S-11 and S-12), as shown by X-ray diffraction.

Vanadium forms covalent bonds with oxygen atoms, similar to phosphorus, and due to its relatively small atomic weight, vanadium–oxygen bonds produce different vibrations in the infrared region. In

TABLE I Chemical composition and experimental conditions for sample preparation

Sample	Chemical composition of lead vanadate (mol %)	La or Fe oxide added (wt %)	Time of heating (h)	Temperature (°C)
S-1	66.7 PbO 33.3 V_2O_5	–	1	800
S-2	50.0 PbO 50.0 V_2O_5	–	1	900
S-3	33.3 PbO 66.7 V_2O_5	–	1	800
S-4	50.0 PbO 50.0 V_2O_5	La_2O_3 (2.5)	1	900
S-5	50.0 PbO 50.0 V_2O_5	La_2O_3 (5.0)	1	900
S-6	50.0 PbO 50.0 V_2O_5	La_2O_3 (10.0)	1	900
S-7	50.0 PbO 50.0 V_2O_5	La_2O_3 (20.0)	1 0.25	900 1150
S-8	50.0 PbO 50.0 V_2O_5	La_2O_3 (25.0)	1	1300
S-9	50.0 PbO 50.0 V_2O_5	Fe_2O_3 (5.0)	1	900
S-10	50.0 PbO 50.0 V_2O_5	Fe_2O_3 (10.0)	1	900
S-11	50.0 PbO 50.0 V_2O_5	Fe_2O_3 (15.0)	1.20	1000
S-12	50.0 PbO 50.0 V_2O_5	Fe_2O_3 (20.0)	1	1100

TABLE II The results of X-ray diffraction phase analysis

Sample	Phase composition (approx. molar fraction)
S-1	$Pb_2V_2O_7$
S-2	Amorphous
S-3	Amorphous
S-4	Amorphous
S-5	Amorphous
S-6	Amorphous + $Pb_2V_2O_7$ (≈ 0.01)
S-7	Amorphous + $Pb_2V_2O_7$ (≈ 0.10)
S-8	Amorphous + $Pb_2V_2O_7$ (≈ 0.05)
S-9	Amorphous
S-10	Amorphous
S-11	Amorphous
S-12	Amorphous

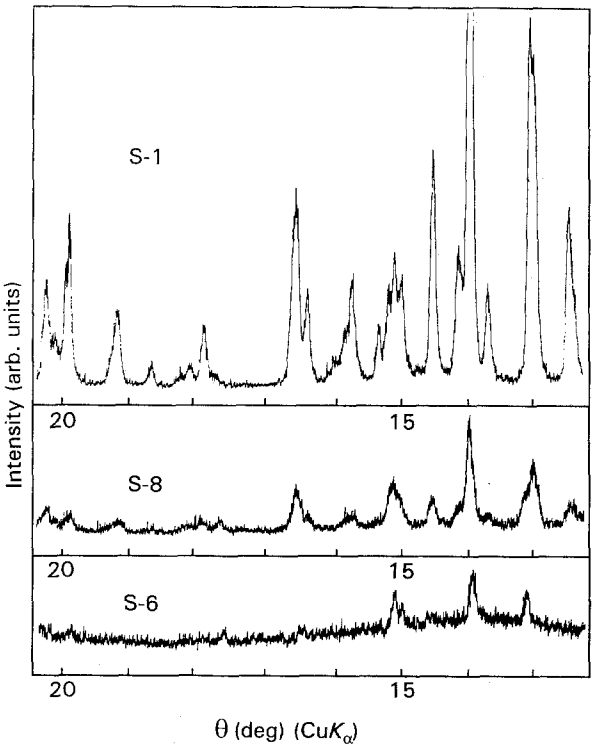

Figure 1 X-ray diffraction patterns of samples S-1, S-8 and S-6, containing crystalline $Pb_2V_2O_7$.

FT–IR spectrum of polycrystalline V_2O_5 (Kemika) is shown in Fig. 2. This spectrum is characterized with strong bands at 1023 and 818 cm^{-1}, and a very strong and broad band with transmittance minima at 574, 531 and 481 cm^{-1}.

Vibrational spectra of V_2O_5 were the subject of several investigations [14–17]. Differences observed in the experimental spectra were generally caused by the state of V_2O_5 (single-crystal, polycrystalline, amorphous). Gilson *et al.* [14] reported IR and Raman bands for V_2O_5 crystal and compared with those obtained on the basis of Kramers–Kronig analysis. Clauws and Vennik [15] measured the reflectance IR spectra on the V_2O_5 single crystal. They also recorded the transmittance IR spectrum for V_2O_5 powder, and measured bands were classified as follows: active IR 262, 370, 472, 813 and 982 cm^{-1} for B_{3u} mode, 1023 cm^{-1} for B_{2u} mode and 217, 294 and 605 cm^{-1} for B_{1u} mode.

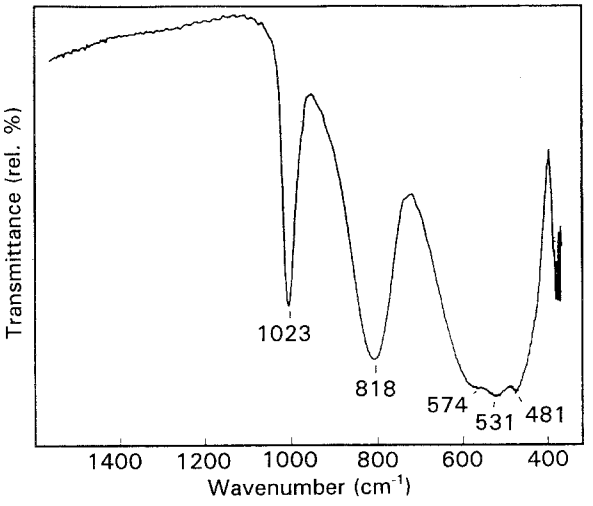

Figure 2 Fourier transform IR spectrum of polycrystalline V_2O_5.

Fig. 3 shows Raman spectrum of polycrystalline V_2O_5 (Kemika). The strongest band at 992 cm^{-1} and a weak band at 1022 cm^{-1} can be ascribed to molecular vibrations, $\nu_S(VO_A)$, of V_2O_5. These bands, as well as others shown in Fig. 3, can be compared with those reported by Abello *et al.* [16]. On the basis of their model, the molecular vibrations were calculated for three kinds of vanadium–oxygen bonds exsisting in V_2O_5 structure, which were denoted VO_A, VO_B and VO_C. The unit-cell representation of V_2O_5 is shown in Fig. 1 of [16]. Abello *et al.* [16] identified three frequency ranges characteristic for V_2O_5. The vibrations associated with VO_A bonds were located at 1000 cm^{-1} for stretching modes and at 155–346 cm^{-1} for bending modes. The vibration modes characteristic of the bridging oxygens VO_BV were located at $\approx$ 830, 450 and 200 cm^{-1}. The asymmetric stretching VO_BV vibration was located at $\approx$ 550 cm^{-1} and associated mainly with the displacement of vanadium atoms. The vibration bands located at $\approx$ 700 cm^{-1}, 535, 487–480 cm^{-1} and 316–387 cm^{-1} corresponded to stretching and bending modes of VO_C bonds, respectively.

Fig. 4 shows FT–IR spectra of samples S-1, S-2 and S-3. The FT–IR spectrum of sample S-1 shows a very strong and broad band with transmittance minima at 874, 834–826, 774 and 698–687 cm^{-1}, as well as a sharp band of medium intensity at 578 cm^{-1}. This spectrum corresponds to lead pyrovanadate. The IR spectra of pyrovanadates, $Cu_2V_2O_7$, $Mg_2V_2O_7$, $Co_2V_2O_7$, $Ni_2V_2O_7$, $Zn_2V_2O_7$, $Cd_2V_2O_7$ and $Mn_2V_2O_7$ were recorded and discussed by Pedregosa *et al.* [18]. Differences between the corresponding IR spectra of metal(II) pyrovanadates were explained by the distortion of $V_2O_7^{4-}$ group, as a consequence of the presence of different metal cations in the crystal lattice. Kristallov *et al.* [19] investigated the correlation between the characteristic IR vibrations and the bridge angle V–O–V in metal(II) pyrovanadates,

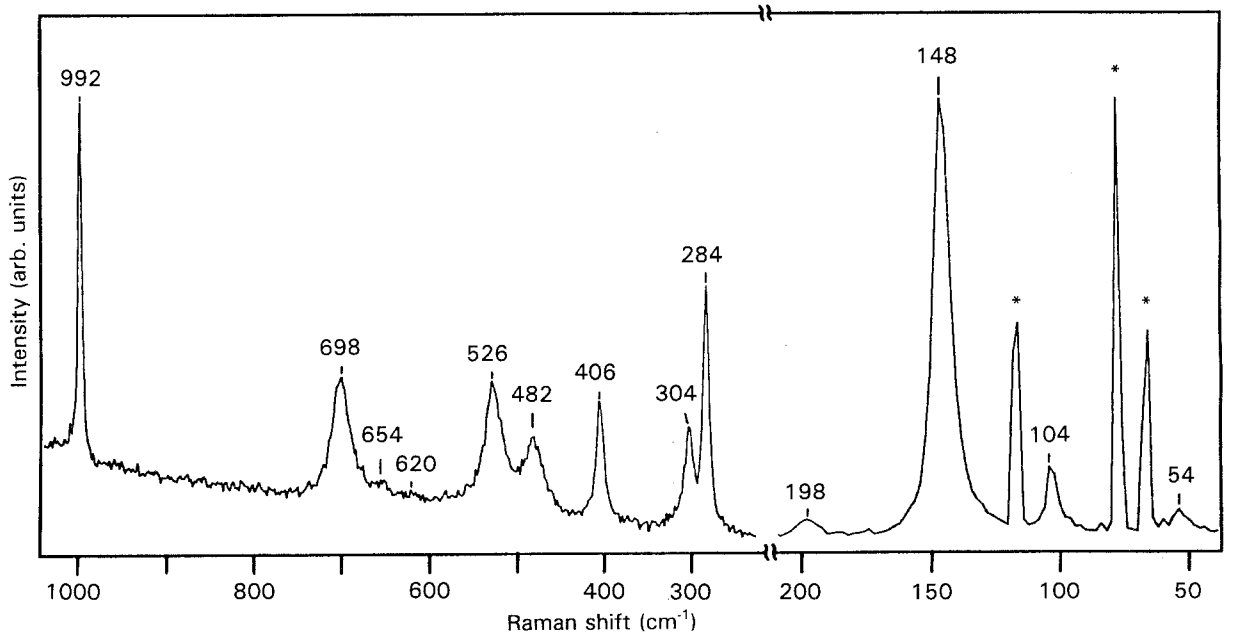

Figure 3 Laser Raman spectrum of polycrystalline V_2O_5. (*) Parasite plasma lines.

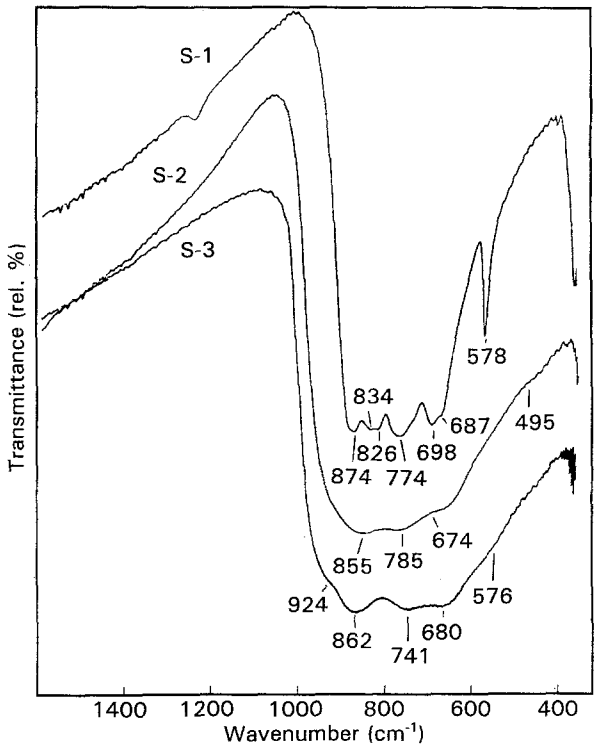

Figure 4 Fourier transform IR spectra of samples S-1, S-2 and S-3.

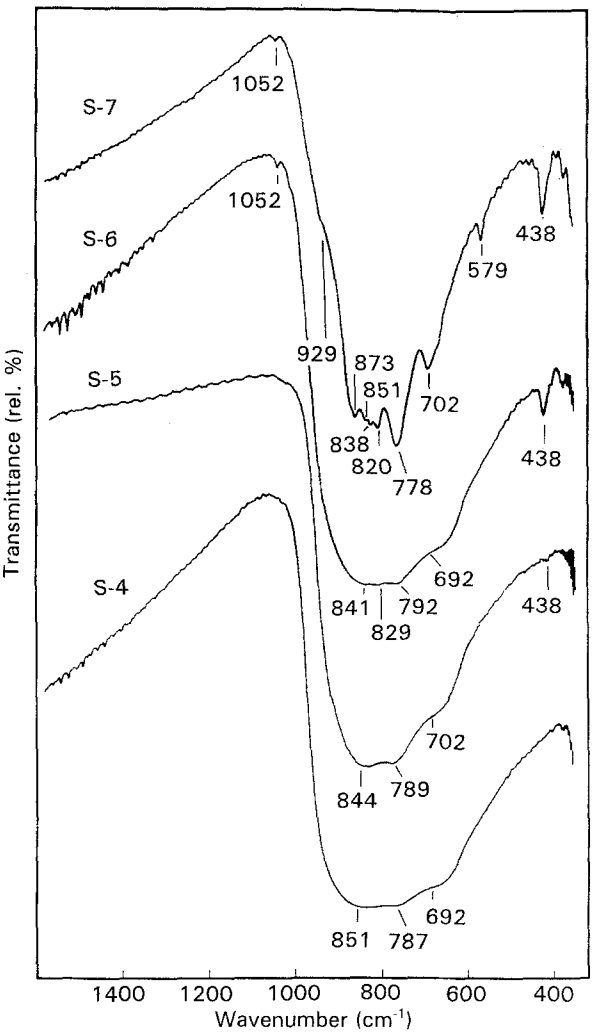

Figure 5 Fourier transform IR spectra of samples S-4, S-5, S-6 and S-7.

$Cd_2V_2O_7$, α-$Zn_2V_2O_7$, β-$Mg_2V_2O_7$, $Ba_2V_2O_7$, $Sr_2V_2O_7$, α-$Mg_2V_2O_7$ and $Ni_2V_2O_7$. The vibrations ν^{as}_{VOV} and ν^{s}_{VOV} were dependent on the bridge angle V–O–V. The wave number, ν^{as}_{VOV}, changed from 730 cm^{-1} for $Cd_2V_2O_7$ to 666–645 cm^{-1} for $Ni_2V_2O_7$, while the wave number of ν^{s}_{VOV} changed from 475 cm^{-1} for α-$Zn_2V_2O_7$ to 582 cm^{-1} for $Ni_2V_2O_7$.

Sample S-2 with metavanadate composition showed a very strong and broad band with peaks at 855, 785 and 674 cm^{-1}, as well as a weak shoulder at 495 cm^{-1}. These peaks were also characteristic for crystalline lead metavanadate; however, in this case they were much better pronounced [20]. With further increase of V_2O_5 content in the system PbO–V_2O_5 (sample S-3), in addition to peaks at 862, 741 and 680 cm^{-1}, two shoulders, at 924 and 576 cm^{-1}, are also visible. The shoulder at 924 cm^{-1} indicates the presence of short isolated V=O bonds. Generally, with the incorporation of metal ion content in V_2O_5 glass and increase of dopant concentration there is gradual shift of the IR band at 1023 cm^{-1} to lower wavenumbers.

Fig. 5 shows changes in the FT–IR spectra of samples S-4, S-5, S-6 and S-7 influenced by the incorporation of La^{3+} in lead metavanadate glass. With the increase of La^{3+} content there is a gradual shift of the band at 855 cm^{-1} for sample S-2 to 841 cm^{-1} for sample S-6. The FT–IR spectrum of sample S-6 also showed the appearance of the band at 829 cm^{-1}. The FT–IR spectrum of sample S-7 is significantly different in relation to the spectra of samples S-4, S-5 and S-6. On the basis of the spectrum of sample S-7, the presence of crystalline $Pb_2V_2O_7$ in the glass matrix can be concluded. The role of the IR band at 438 cm^{-1} should be emphasized. The intensity of this band at 438 cm^{-1} is very weak in the FT–IR spectrum of sample S-5. With a further increase of La^{3+} content in the glass, there is a gradual increase of the intensity of the band at 438 cm^{-1}, and this can be attributed to the presence of $LaVO_4$ in the glass matrix. Baran and Aymonino [21] observed, in the IR spectrum of $LaVO_4$, the vibration $\nu_4(VO_4^{3-})$ at 432 cm^{-1}. These authors [22] also recorded $\nu_4(VO_4^{3-})$ frequency for $CeVO_4$ at 442 cm^{-1}, for $PrVO_4$ at 441 cm^{-1}, for $NdVO_4$ at 443 cm^{-1}, for $SmVO_4$ at 445 cm^{-1}, for $EuVO_4$ at 443 cm^{-1} and for $GdVO_4$ at 448 cm^{-1}. Yamaguchi *et al.* [23] prepared YVO_4 by the sol–gel procedure, and the IR spectrum of this compound showed vibrations $\nu_1(VO_4^{3-})$ at 870 cm^{-1}, $\nu_3(VO_4^{3-})$ at 820 cm^{-1}, $\nu_4(VO_4^{3-})$ at 430 cm^{-1} and $\nu_2(VO_4^{3-})$ at 350 cm^{-1}. In order to gain additional evidence for the presence of $LaVO_4$, the laser Raman spectra were recorded. Fig. 6 shows laser Raman spectra of samples S-1, S-7 and S-8. The most important difference observed in relation to the spectrum of sample S-1 ($Pb_2V_2O_7$) is the appearance of the peaks at 856 cm^{-1} for sample S-7 and 854 cm^{-1} for sample S-8. From the literature [21] it is known that the Raman spectrum of $LaVO_4$ showed the most prominent peak at 860 cm^{-1}, which can be ascribed to $\nu_1(VO_4^{3-})$.

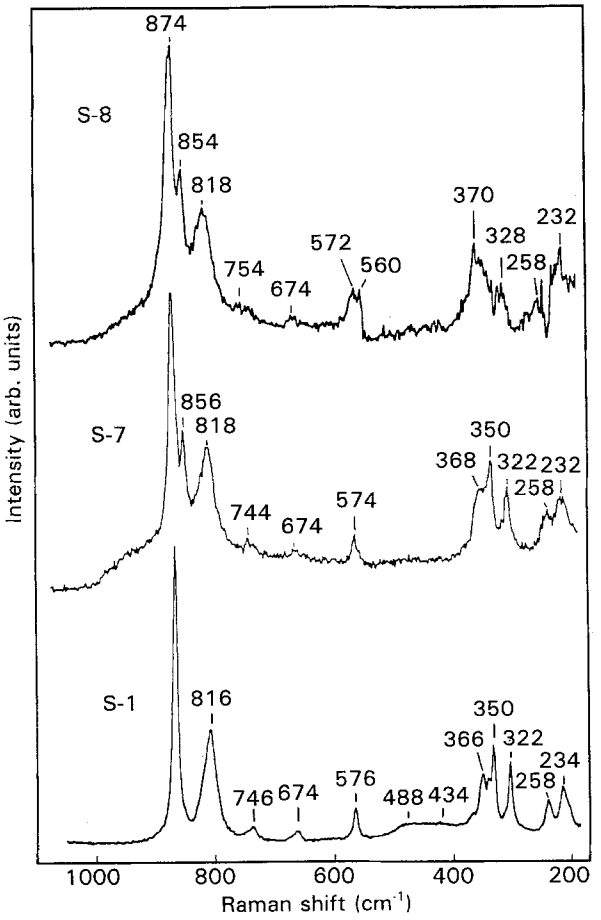

Figure 6 Laser Raman spectra of samples S-1, S-7 and S-8.

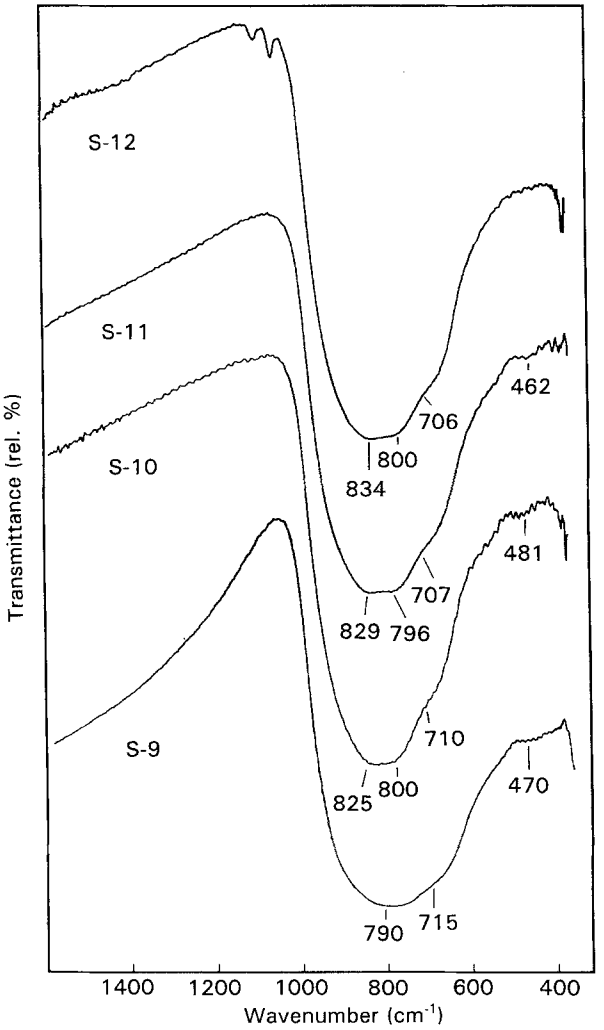

Figure 7 Fourier transform IR spectra of samples S-9, S-10, S-11 and S-12.

Fig. 7 shows FT–IR spectra of samples S-9 to S-12. These spectra are very similar and on the basis of their shape it can be suggested that samples S-9 to S-12 are glasses. XRD analysis confirmed their glassy state. The main characteristics of these spectra is a flattening of the band at 790 cm^{-1} observed for sample S-9 and a disappearance of a weak band at $\approx 470\ cm^{-1}$ in the spectrum of sample S-12. Evidently, the influence of La^{3+} and Fe^{3+} cations on the structural properties of lead metavanadate glass is different. For the same molar fractions of dopants more glass component was obtained for Fe^{3+} than for La^{3+}. It is likely that Fe^{3+} cations easily replace V^{5+} and this can be attributed to similar ionic radii of Fe^{3+} (0.064 nm) and V^{5+} (0.059 nm).

Nishida *et al.* [24] investigated the structure of Na_2O–V_2O_5 glasses containing 10 mol% Fe_2O_3. Tetrahedral coordination of Fe^{3+} was determined by Mössbauer spectroscopy. The authors concluded that incorporation of Na_2O into the V_2O_5 matrix caused a gradual change from the layer structure, built of the V_2O_5 tetragonal pyramids (or trigonal bipyramids), to the chain structure, built of the VO_4 tetrahedra having non-bridging oxygen atoms. Nishida *et al.* [25] also investigated the structure of Li_2O–, MgO–, and BaO–V_2O_5 glasses containing 10 mol% Fe_2O_3. It was found that Fe^{3+} ions were tetrahedrally coordinated with oxygen atoms at the substitutional sites of V^{5+} or V^{4+} ions. Incorporation of Li_2O into the V_2O_5 matrix caused structural changes similar to those observed for Na_2O–V_2O_5 glasses. On the other hand, it was concluded that incorporation of MgO or BaO into the V_2O_5 matrix resulted in a gradual change of the original layer structure built of VO_5 tetragonal pyramids to the highly complicated three-dimensional network structure built of VO_4 tetrahedra.

Structural changes of the glasses formed in the system Fe_2O_3–V_2O_5 were investigated by IR spectroscopy [26]. It was established that the short-range order of glasses in the system Fe_2O_3–V_2O_5 was similar to that of the corresponding crystalline phases. The main structural constituents in vitreous $FeVO_4$ are VO_4 tetrahedra. A transformation of the VO_5 tetragonal pyramids into VO_4 tetrahedra takes place as the fraction of Fe_2O_3 increases, with formation of $FeVO_4$.

References

1. A. A. FOTIEV, B. V. SLOBODIN and M. YA. KHODOS, "Vanadates, Composition, Synthesis, Structure, Properties" (Nauka, Moscow, 1988) 272 pp. (in Russian).
2. V. A. GUBANOV, D. E. ELLIS and A. A. FOTIEV, *J. Solid State Chem.* **21** (1977) 303.
3. M. SAYER and A. MANSINGH, *Phys. Rev.* **B6** (1972) 4629.
4. A. TSUZUKI, S. KAWAKAMI, M. AWANO, T. SEKIYA and Y. TORII, *J. Mater. Sci. Lett.* **7** (1988) 745.

5. E. SUONINEN, E. MINNI and I. M. CURELARU, *J. Microsc. Spectrosc. Electron.* **6** (1981) 1.
6. G. CALESTANI, A. MONTENERO, F. PIGOLI and M. BETTINELLI, *J. Solid State Chem.* **59** (1985) 357.
7. B. V. SLOBODIN, V. A. ZHILYEV, N. V. KISELEVA, Y. N. BLINOVSKOV, *Zh. Neorg. Khim.* **31** (1986) 268.
8. G. CALESTANI, G. D. ANDREETTI, A. MONTENERO and M. BETTINELLI, *Acta Crystallogr.* **C41** (1985) 177.
9. G. CALESTANI, G. D. ANDREETTI, A. MONTENERO M. BETTINELLI and J. REBIZANT, *ibid.* **C41** (1985) 179.
10. B. D. JORDAN and C. CALVO, *Can. J. Chem.* **52** (1974) 2701.
11. E. BAIOCCHI, M. BETTINELLI, A. MONTENERO and L. D. SIPIO, *J. Solid State Chem.* **43** (1982) 63.
12. F. MOMO, A. SOTGIU, E. BAIOCCHI, M. BETTINELLI and A. MONTENERO, *J. Mater. Sci.* **17** (1982) 3221.
13. E. AGOSTINELLI, P. FILACI, D. FIORANI, A. MONTENERO and M. BETTINELLI, *J. Non-Cryst. Solids* **84** (1986) 329.
14. T. R. GILSON, O. F. BIZRI and N. CHEETHAM, *J. Chem. Soc. Dalton* (1973) 291.
15. P. CLAUWS and J. VENNIK, *Phys. Status Solidi (b)* **76** (1976) 707.
16. L. ABELLO, E. HUSSON, Y. REPELIN and G. LUCAZEAU, *Spectrochim. Acta* **39A** (1983) 641.
17. C. SANCHEZ, J. LIVAGE, J. P. AUDIERE and A. MADI, *J. Non-Cryst. Solids* **65** (1984) 285.
18. J. C. PEDREGOSA, E. J. BARAN and P. J. AYMONINO, *Z. Anorg. Allg. Chem.* **404** (1974) 308.
19. L. V. KRISTALLOV, A. A. FOTIEV, L. A. PERELYAEVA and M. P. CVETKOVA, *Zh. Neorg. Khim.* **30** (1985) 3202.
20. V. DIMITROV and Y. DIMITRIEV, *J. Non-Cryst. Solids* **122** (1990) 133.
21. E. J. BARAN and P. J. AYMONINO, *Z. Anorg. Allg. Chem.* **383** (1971) 220.
22. *Idem, ibid.* **383** (1971) 226.
23. O. YAMAGUCHI, Y. MUKAIDA, H. SHIGETA, H. TAKEMURA and M. YAMASHITA, *Mater. Lett.* 7 (1988) 158.
24. T. NISHIDA, M. OGATA and Y. TAKASHIMA, *Bull. Chem. Soc. Jpn* **60** (1987) 2887.
25. T. NISHIDA, S. SARUWATARI and Y. TAKASHIMA, *ibid.* **61** (1988) 2343.
26. V. DIMITROV, Y. DIMITRIEV and V. MIHAILOVA, *Monatsh. Chem.* **114** (1983) 669.

Received 7 August 1992
and accepted 12 August 1993